Characterization of Surface Fault Patterns with Application to a Layered Manufacturing Process [1]

Irem Y. Tumer, David C. Thompson, Kristin L. Wood, Richard H. Crawford,
Mechanical Engineering Department, The University of Texas at Austin, Austin, Texas

Abstract

Detection of faults is a continuing need in all manufacturing processes. This need is more pronounced in new manufacturing processes where continual product improvement is desired. In this paper, a systematic approach is developed for addressing this need. Contemporary experimental and surface analysis techniques provide a basis for incrementally diagnosing the fault mechanisms leading to surface deviations. Based on this general approach, a maturing layered-manufacturing process is investigated, notably, Selective Laser Sintering (SLS). We first show through experimental analysis that layer-thickness and part orientation affect surface quality. Using these experimental results, random-process analysis is carried out to determine the specific fault patterns. The quantification of these fault patterns leads to the identification of fault sources, which provide a foundation for monitoring and control. The paper concludes with a summary of fault mechanisms on SLS parts, implementation issues for improving part quality, and insights for applying our approach to other manufacturing processes.

Introduction

In most manufacturing processes, the variables and mechanisms to monitor and control are known in advance: methods to diagnose faults that result in poor part quality rely on previous knowledge of fault patterns, using either known patterns, models, or predetermined specifications and control limits [1, 2]. However, when a newly-developed manufacturing process is being investigated, the nature of the fault patterns is not known [2]; trial and error is often used until acceptable parts are produced and rules-of-thumb are gathered to pass on to the next operator.

In this work, we aim to eliminate the need for pre-existing knowledge of the nature of faults in the production of high-quality parts and present methods that can be applied systematically to detect and diagnose faults that affect part quality. In this light, an approach is presented to investigate the effect of changes in process parameters and to isolate the fault patterns that result in poor surface quality. We present a formal means to quantify and characterize the significant parameters and fault patterns. Once these are identified, monitoring and control tools, along with optimization schemes, can be implemented to assure the production of high quality parts.

A number of techniques exist for analyzing part quality. Such techniques include experimental design, surface analysis, and random-process analysis. While these techniques are used extensively, very few integrated approaches exist, especially for diagnosing newly developed manufacturing processes. The need thus exists for an efficient and systematic approach for diagnosing the faults that degrade part quality [3].

In this work, the following approach is proposed to investigate faults in a newly-developed manufacturing process:

1. Select desired system response in the manufacturing process;

[1] This paper is published in The Journal of Manufacturing Systems, Vol. 17, No.1

2. Apply physical insight to select a subset of significant mechanisms and parameters in the process;

3. Setup experiments and apply experimental design and analysis;

4. Determine average characteristics and trends based on experimental results;

5. Determine the nature of fault patterns with random process analysis;

6. Choose remedial actions for monitoring and control.

The steps of this approach are selected carefully to gain incremental insights into fault detection. These steps also provide latitude for choosing different analysis techniques, depending on the nature of the system response and fault patterns.

The diagnostic approach is implemented in the context of a maturing layered manufacturing process, namely, Selective Laser Sintering. Surfaces built using this process are analyzed to determine parameters and mechanisms that potentially affect product quality. However, the methods used in this paper and the proposed approach can be applied to the diagnosis of any new manufacturing process. Using the approach, the significant parameters that affect part quality are first established within a feasible parameter space. Then, the fault mechanisms are isolated and characterized; these mechanisms can be monitored individually in order to eliminate the origin of the faults. The results of the phenomenological study of surface fault mechanisms will provide a means of developing an error budgeting scheme. Such schemes are commonly provided in the literature for known error types [4].

Selective Laser Sintering

The manufacturing process under study is Selective Laser Sintering (SLS). The following sections describe the process and discuss the physical insights which lead to the investigation of fault mechanisms in SLS. These descriptions embody the first two steps of our diagnostic approach.

Selection of System Response: Background and Motivation

Selective Laser Sintering [5] is one of the leading rapid prototyping processes used to produce functional prototypes [6]. Functional prototyping, a major advantage of the SLS process, depends heavily upon the ability to build accurate, high quality parts on a repeatable basis [7, 8]. A possible application of functional prototyping parts are polymer connectors, whose mating surfaces have to satisfy high quality conditions.

The quality of parts from SLS has been investigated in the literature in terms of system responses such as overall part dimensions [9], part strength [10], and sintering depth and density [11]. These studies give a broad picture in order to present operators with a set of preferred parameters when building SLS parts. However, none of these studies attempt to provide insight on why surface deviations occur on SLS parts and what fault patterns affect surface quality [12]. Part quality, for this paper, is thus defined in terms of surface deviations on SLS parts, resulting in fault patterns.

As in every manufacturing process, the finished part is the end product that satisfies the customer needs. The nature of the signal from surfaces of manufactured parts contains very useful information that can provide great insight into the types of patterns present in the system [13]. As a

result, an investigation of signals from polycarbonate SLS part surfaces will provide an understanding of the nature of fault generating mechanisms in SLS. Polycarbonate (average particle diameter of 70 μm), a thermoplastic powder material, is used because of its high demand for producing prototypes.

Description of the Process

The SLS process is based on the system depicted in Figure 1 [6]. The powder delivery system deposits a thin layer of powder onto the work surface from the powder cylinder. A roller mechanism spreads the powder evenly, and a computer-controlled laser beam scans the surface of the powder layer to the desired shape by means of scanners and mirrors. The beam is turned on and off to heat up and sinter the powder in the selected areas to be occupied by a part at a given cross-section. Successive layers of powder are deposited and sintered until the entire part is produced. In areas not sintered, powder is loose and is removed when the part is complete.

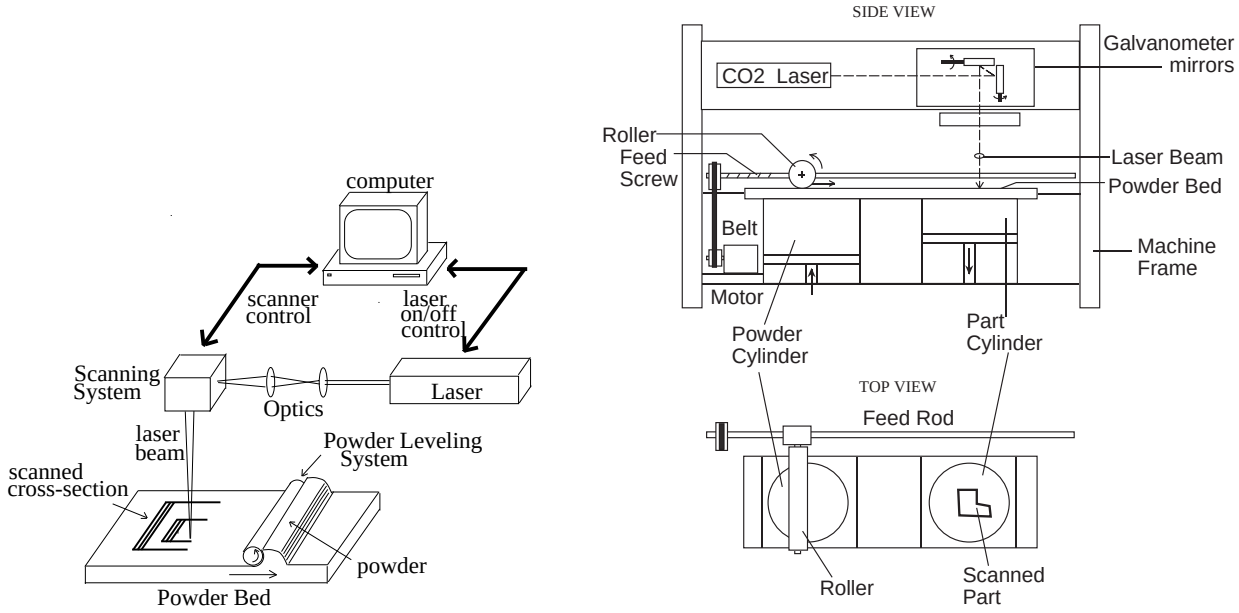

(a) The Overall Process.

(b) A Detailed Schematic of the Machine.

Figure 1: The Selective Laser Sintering Machine Process.

Identification of Fault Generating Mechanisms in SLS

In any manufacturing system, there is a subset of parameters and mechanisms that potentially affect the quality. In this work, we start with the assumption that we do not know these parameters and mechanisms. Our purpose is to detect and identify the fault mechanisms that degrade surface quality. The first step in such an investigation is to gather all physical insight about the manufacturing process under study.

The physical mechanisms that have the potential to generate faults on final SLS parts can be divided into four main categories: (1) faults caused by the machine's dynamic response, (2) faults from the system's thermal response, (3) faults due to the part's geometry and orientation in the powder bed, and (4) faults caused by the surface texture as a result of the size, shape, distribution, and sintering properties of the powder material. In order to reveal a subset of these submechanisms, this study focuses on the surfaces of experimentally-built SLS parts. These surfaces should ideally reflect the combined effect of the laser mechanism, roller mechanism, the scanning mechanism, as well as the effect of depositing multiple layers of powder composed of spherical particles. Each of these mechanisms, as well as their potential interactions, may result in the generating of specific fault mechanisms on the part surfaces. This paper aims to identify the parameters and mechanisms that degrade surface quality.

Experimental Design and Analysis of Surface Quality

In this section, steps 3 and 4 of the diagnostic approach are implemented to study the average surface characteristics of SLS parts. One subset of parameters which are identified as potentially affecting part quality consists of layer thickness, laser power, and part orientation. These parameters are operator controllable; their values are typically set by trial-and-error and calibrated regularly to produce the best part possible. This section describes a set of experiments and an experimental analysis method, designed to test the significance of these experimentally controlled parameters in producing quality SLS surfaces. As such, it represents a crucial step in acquiring the necessary data to analyze the fault patterns incrementally. A similar experimental study can be conducted on different subsets of parameters.

Selection of Parameters and Their Ranges

The parameters varied in the experiments are laser power, P, layer thickness, l_t, and build angle, θ_b. Laser power determines the severity of temperature gradients which introduce deviations due to thermal modes on parts. In addition, the laser power is the mechanism by which melting and sintering of the powder particles is initiated. As a result, the level of the power is a significant contributor the the surface quality. Layer thickness affects the quality of the surfaces that are approximated due to the layer-forming property of SLS, creating an irregular pattern on angled surfaces. Orientation is also a major factor in affecting the quality of surfaces formed by the same approximation. Orientation is quantified in terms of build angle. Build angle is the angle between the part's longitudinal axis and the horizontal plane of the powder bed.

The ranges for each parameter are shown in Table 1. The feasible parameter space and the ranges of the parameter values are chosen based on the practical considerations for laser power and layer thickness [14]. The range for part orientation is chosen so that surfaces built at an angle can be compared to the best surfaces obtained from horizontally-built parts; as a result, part orientation is varied from 0 to 90°. A 45° angle is chosen to represent angled surfaces for the factorial approach used in this work. In addition, parts are also built at intermediate angles of 30° and 60° in order to further study the severity and magnitude of surface errors introduced by changing the angle.

Table 1: Parameters and their ranges.

Parameter	Low	Medium	High
Power, $P = X_1$	10 $[W]$	–	15 $[W]$
Layer Thickness, $l_t = X_2$	127 $[\mu m]$	–	178 $[\mu m]$
Build Angle, $\theta_b = X_3$	0 $[deg]$	45 $[deg]$	90 $[deg]$

Design of Experiments

For the purposes of determining the effect of process parameters on part quality, a factorial experimental design is used. This experimental method affords us with a general representation of the surface quality response for the manufacturing process, thus providing quality bounds. Other experimental methods exist, such as surface response methodology [15]; the key in choosing an appropriate method in our diagnostic approach is to have the ability to search the entire response space. A factorial design satisfies this requirement for the SLS process, implying that in each complete trial of the experiment, all relevant combinations of the levels of the factors are investigated [16]. Furthermore, the factorial design approach provides a means of monitoring the experimental error. To obtain significant results, we want to assure that the effects of the design parameters are greater than the experimental error.

Because of the time required to perform the experiments, each run includes a tensile specimen (Figure 2(a)) at every build angle in the test, plus two in-betweens, which are produced mainly for verifying the resulting model of the upcoming analysis. The layout of parts in the bed is shown in Figure 2(b). Two data points (i.e., two replicates) are taken at each trial level because this is the minimum number required to obtain an estimate of variance for each trial. Wolf and Tauber's [17] principle indicates this should be adequate for showing an effect is significant to within one standard deviation, σ, the experimental error. Since each run includes every build angle level, only four runs are required for each replicate. Each replicate is performed in a random order, with one run per day. To evaluate the data obtained, an analysis of variance (ANOVA) study is performed. This analysis

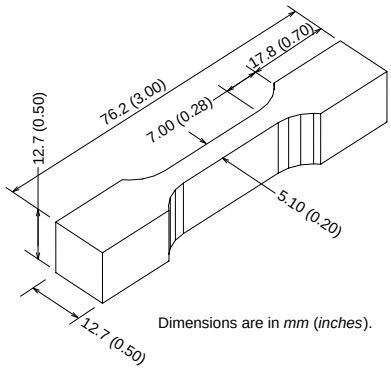

(a) Tensile specimen geometry.

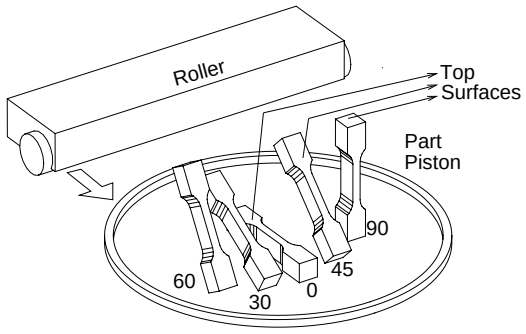

(b) Layout of parts in the part piston.

Figure 2: Tensile Specimen Dimensions and Layout.

fits a polynomial surface to the experimental data and then discards terms that are statistically insignificant [16].

Results and Observations from Experiments

Polycarbonate powder is used to form small test specimens, each 76.2 mm (3 $in.$) long with square cross-sections of 12.7 mm (0.5 $in.$) at the ends, as shown in Figure 2(a). The tensile specimen is a standard test part commonly used in SLS studies. A contact profilometer [18] is used to obtain profiles of the surfaces facing upwards on the powder bed. Since we are currently interested in studying the dynamic effects of the laser and the roller mechanisms on the top layers, measurements are obtained on the "top" surfaces of the test specimens only, as indicated in Figure 2(b). These surfaces provide the maximum amount of information for each part. Measurement of the remaining surfaces indicates that no new information is added. The output of interest for each test in these experiments is the RMS surface roughness, shown in Table 2. The results from these experiments are shown in Table 2. Here, R_q refers to the RMS average roughness of the measured surfaces, X_1 is the laser power effect, X_2 is the layer thickness effect, and X_3 is the build angle effect.

Table 2: Experimental conditions and results.

Test	Run	X_1	X_2	X_3	R_q $[\mu m]$	
					Rep.I	Rep.II
1		-1	-1	-1	34.4	34.8
2	A1, A2	-1	-1	0	31.4	36.1
3		-1	-1	1	23.3	27.1
4		-1	1	-1	35.0	35.0
5	B1, B2	-1	1	0	47.2	46.6
6		-1	1	1	30.4	31.7
7		1	-1	-1	41.2	43.7
8	C1, C2	1	-1	0	32.9	32.5
9		1	-1	1	25.0	22.0
10		1	1	-1	34.9	43.9
11	D1, D2	1	1	0	43.6	39.7
12		1	1	1	30.9	29.0

Applying the factorial design in Table 2 [16], the manufactured parts are assessed qualitatively to determine the general trends of fault patterns. For the SLS experiments, observations of the manufactured parts indicate several patterns that we had not anticipated. For example, the top surfaces of the parts show significant melting, especially apparent in parts produced at high power levels. In addition, parts produced at an angle show a peculiar pattern due to a shifting of the layers observed during the process, again emphasized on parts built at high power levels. We observed that the layers are shifted due to the roller motion; some of the initial layers are dragged back and forth on the loose powder bed as the roller deposits a new layer of powder. The question that remains is whether we can detect these patterns (and any others that may exist) by the surface analysis methods and quantify their severity.

Characterization of SLS Parts with Surface Quality Measures

Mathematical measures are necessary to detect and quantify the significance of faults on manufactured surfaces. In this section, the effect of the experimentally controlled parameters on the overall surface deviations is determined. Surface analysis is often used to study the irregularities in surface geometry, which provide a "fingerprint" of the manufacturing process [13, 19]. Specifically, profile parameters are used to characterize surface quality, such as average roughness and waviness parameters. Average profile parameters represent suitable measures to aid communication between engineers and the production floor [13].

The geometric average R_q (RMS roughness) height measure is a standard approach for communicating the desired surface precision [13]. This average measure is computed from the filtered roughness signals from top surface measurements as follows [18]:

$$R_q = \sqrt{\frac{y_1^2 + y_2^2 + ... + y_n^2}{n}} \tag{1}$$

where y_i are the height measurements, and n is the total number of sample points. In this study, the RMS roughness measure R_q is used instead of the arithmetic average R_a because of its higher reliability [13].

Profile measurements are made along the long axis of the tensile specimen (Figure 2), on the face pointing "upwards," over a traverse length of 40 mm, with a cutoff evaluation length of 2.5 mm. The 90°-oriented parts are measured using a traverse length of 10 mm. A total traverse length of nominally five cutoff lengths is deemed appropriate to evaluate the average roughness parameters accurately [13]. For the case of a 10 mm traverse length, a cutoff length of 0.8 mm was shown to result in approximately the same roughness value as a cutoff length of 2.5 mm. As a result, a constant cutoff length of 2.5 mm was used for both traverse lengths. Measurement of the longer surfaces using varying traverse lengths (5 mm, 10 mm, 20 mm, 40 mm) shows negligible natural variations of the RMS roughness along the surfaces. In addition, profile measurement at different locations along the SLS parts indicates a consistent roughness value throughout the surface. The results are shown in Table 2. The effect of laser power, layer thickness, and build angle on surface quality is investigated by means of ANOVA; the results are shown in Table 3. Here SS stands for sum of squares, DOF is the degrees of freedom, MS is the mean squared error equal to SS/DOF, and F ratio is the test statistic equal to the ratio of MS for each term and the MS for error [16]. For a 99% level of confidence, an F-test comparing the contribution of an effect to that of the pure error must be above $F_{.01,1,12} = 9.33$ [16].

The resulting regression model from ANOVA is given by:

$$y = 38.72 + 5.544X_2 - 5.222X_3 - 6.097X_3^2 + 2.741X_1X_3^2 - 4.347X_2X_3^2. \tag{2}$$

where y is the surface roughness, X_1 is the laser power effect, X_2 is the layer thickness effect, and X_3 is the build angle effect. This qualitative model shows that surface roughness has a tendency to increase with layer thickness (positive effect) and decrease with build angle (negative effect). An increase in surface roughness implies a decrease in surface precision, and hence part quality. In addition, a nonlinear variation of surface roughness with build angle is observed, indicated by the quadratic term in the model. This nonlinear variation is also affected by the interactions of part orientation with layer thickness and laser power. To verify the model, a lack of fit test and residual analysis are performed [20]. The sum of squares of the residual is less than the sum of the squares of the pure error. Thus, there is no lack of fit [7].

Table 3: Roughness ANOVA results.

Source	SS	DOF	MS	F
Main Effect X_1	59.06	1	59.06	9.00
Main Effect X_2	737.60	1	737.60	115.00
Main Effect X_3	436.30	1	436.30	68.00
Interaction Effect X_1X_2	26.15	1	26.15	4.07
Interaction Effect X_1X_3	56.81	1	56.81	8.84
Interaction Effect X_2X_3	55.69	1	55.69	8.66
Interaction Effect X_3^2	594.80	1	594.80	92.50
Interaction Effect $X_1X_3^2$	120.20	1	120.20	18.70
Interaction Effect $X_2X_3^2$	302.30	1	302.30	47.00
Interaction Effect $X_1X_2X_3$	4.05	1	4.05	0.63
Interaction Effect $X_1X_2X_3^2$	7.63	1	7.63	1.19
Within Error	77.13	12		

Determination of Qualitative Trends in Surface Quality

These results conclude the first portion of our approach: having identified surface quality as the quality measure of interest, experimental methods and an analysis of variance technique are applied in order to vary selected parameters and determine their significance. The experimental parameters are selected based on potential error mechanisms. Characteristic measures are then selected and used to develop a qualitative ANOVA model of surface roughness with respect to the selected parameters. The results so far provide us with insight on how the process parameters affect surface precision. The same approach can be used to study other subsets of parameters. One candidate is the scanning subsystem [21]; using a similar approach, we can determine the effects of scanning parameters on surface quality.

Ultimately, if the set of parameters affecting surface precision are monitored, and their respective ranges are known, their values can be re-adjusted to improve a part's surface precision. However, monitoring an average single value such as the surface RMS roughness can often lead to false or incomplete conclusions about the surface precision [22, 13]. For example, two profiles with different frequency fault patterns with similar amplitude values will result in similar average height values even though the fault mechanisms are completely different. Furthermore, although an increase in the average profile parameters will indicate the occurrence of a fault pattern, this information is typically not enough to determine the severity of the fault pattern, the specific location, or the character of the fault pattern. An average profile measure will indicate the steady-state values of the faults on the part surface, and not the onset of the problem. This is crucial information necessary to detect potential problems and failures in the system. Additional knowledge of the character, or shape of the fault pattern is often necessary to determine the source of the fault causing a change in surface precision.

In this light, the following presents a study of the specific effects discovered in this section of the paper. Specifically, the top layers of the 0° and 45° parts are further analyzed to determine the nature of the fault mechanisms that affect surface quality. To obtain the necessary information about the severity and nature of the fault patterns, surface analysis methods using random process analysis tools are typically preferred over the single-value measure approach [13]. These methods

are used next to study signals from manufacturing to gain insight on the nature of the fault patterns that result in poor surface precision.

Characterization of Surfaces by Random Process Analysis

The second part of our approach (steps 5 and 6) involves the investigation of the specific fault patterns on manufactured parts. Random process analysis methods are used to treat the surface profiles as a combination of deterministic and stochastic signals. These methods decompose complex signals into decorrelated individual fault components. The type and origin of the individual fault patterns can then be determined based on the individual fault patterns, and remedial action can be taken if the faults are deemed severe.

Motivation

Surface analysis relies on the assumption that the surface geometry irregularities can be used as a "fingerprint" of the manufacturing process [23, 13]. The slightest change in the process parameters, and in the condition of the machine tool, will manifest itself as changes in surface geometry, in size, texture, form, or a combination.

The need for parameters which are capable of extracting the most useful information from a surface leads to the application of random process techniques to surface analysis [13]. For example, when monitoring the vibration in a system, a technique which enables not only the onset of vibration to be detected, but also the character of vibration, so that the mode of vibration can be detected, is required [19]. This ability of a technique to detect "structures" (e.g., periodicities) in surface signals has to be carried out in the presence of random extraneous noise, and in some cases, the random effects which are characteristic of the manufacturing process, such as in grinding.

In Search of Fault Patterns on SLS Surfaces

As an initial inspection of the signal content, SLS surface measurements are analyzed using spectral analysis [24, 13]. Measurements are performed both on parts that are built horizontally with respect to the build plane (0°), and on parts that are built at an angle with respect to the build plane (45°), as shown in Figure 2(b). Coherent fault patterns will manifest as distinct frequency components in the power spectrum. The frequency at which the fault pattern occurs indicates the existence and character of the fault; whereas, the amplitude of the frequency component indicates the severity of the fault.

Mathematical Basis

Random process analysis implements correlation and spectral-based analysis techniques. The frequency decomposition of a signal can be obtained by using the power spectrum [24, 25]. The power spectrum is a plot of the magnitude squared of the discrete Fourier transform of a signal [13]. Strictly speaking, the Fourier transform of a random process $x(t)$ does not exist, since the random process is of infinite duration and, hence, not absolutely integrable [24]. The appropriate approach is to compute the Fourier transform of the correlation function $R(t,\tau) = E[x(t)x^*(t-\tau)]$, where $E[\,]$ is the expectation operator, since the correlation function is absolutely integrable as a result of the correlation function decaying towards zero as τ becomes very large. The Fourier transform

of the correlation function corresponds to the power spectral density function, which describes how the power in a signal is distributed over frequency. To improve the accuracy of the power spectrum for finite length data with random noise, an estimate of the power spectrum is computed by ensemble-averaging over M different segments of the data. After the symmetry conditions have been taken into account, the discrete version of the power spectrum estimate, based on the discrete Fourier transform, is given as:

$$PS[l] = \begin{cases} \frac{2}{M}\sum_{k=1}^{M} |X^{(k)}[l]|^2 & \text{l=1,2,..}\frac{N}{2}\text{-1} \\ \\ \frac{1}{M}\sum_{k=1}^{M} |X^{(k)}[l]|^2 & \text{l=0,}\frac{N}{2} \end{cases} \tag{3}$$

where the discrete Fourier transform (DFT) of the kth realization of N sample points is defined as:

$$X^{(k)}[l] = \frac{1}{N}\sum_{n=0}^{N-1} x^{(k)}[n] exp(\frac{-i2\pi ln}{N}) \tag{4}$$

and where $x^{(k)}[n]$ is the sampled version of each realization, l is the discrete frequency, N is the number of sample points in each realization, and M is the number of realizations used for the ensemble average shown in Equation 3.

Fault Patterns on Top Surfaces of 0° Parts

Spectral analysis is first performed on the top surface measurements of the 0° SLS parts (Figure 2(b)). The results of this analysis show that thermal patterns and particle characteristics mask the remaining patterns on the measurement of the top surfaces of 0° polycarbonate parts. The resulting power spectrum indicates a predominantly random structure on these surfaces. Specifically, the fault patterns caused by the machine dynamic errors are obscured by patterns such as excessive flow from melting of the powder and the distribution of the powder particles. In general, polycarbonate powder is known to exhibit excessive viscous flow, which contributes to melting. Potential mechanisms masking the nature of faults on part surfaces are summarized in Figure 3.

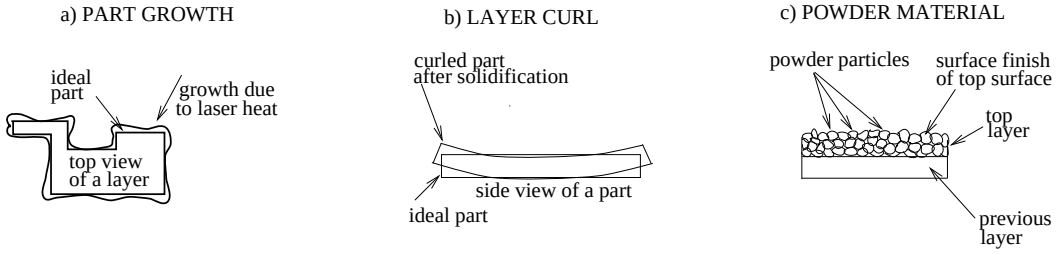

Figure 3: Masking Mechanisms On Parts with Rough Polycarbonate Material.

To search for the fault patterns that are masked by the powder characteristics, a similar test part made using a finer powder product is used to analyze the top surfaces of 0° parts. The finer powder product is similar to the standard polycarbonate powder, but with smaller particles of more spherical shape; these are two properties that eliminate the problem we encountered using the standard polycarbonate powder. A picture of the surface of such a part, along with a picture

of the top surface of a standard polycarbonate part, are shown in Figure 4. Notice that a wavy pattern can be observed on the test part built with finer particles (Figure 4(b)), whereas no coherent patterns are observed on the previous experimental parts (Figure 4(a)).

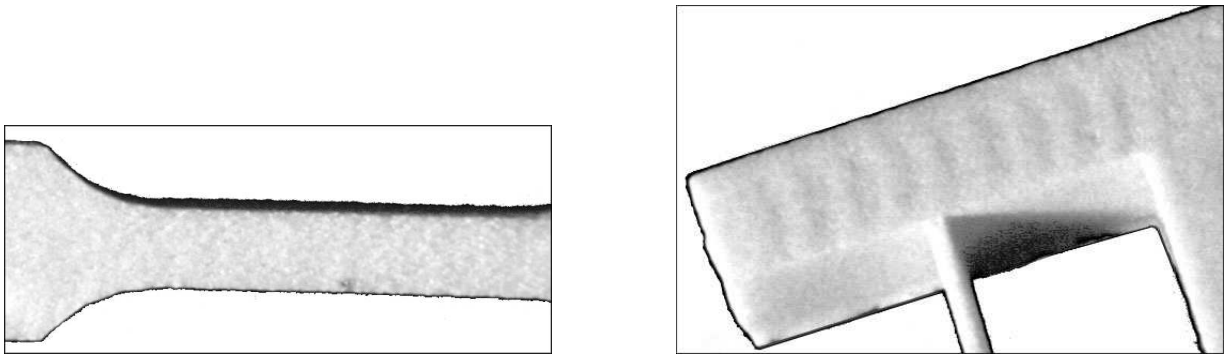

(a) Experimental Part Using Rough Particles (top surface).

(b) Test Part Using Finer Particles (top surface).

Figure 4: Surface Pictures: Rough vs. Finer Particle Material.

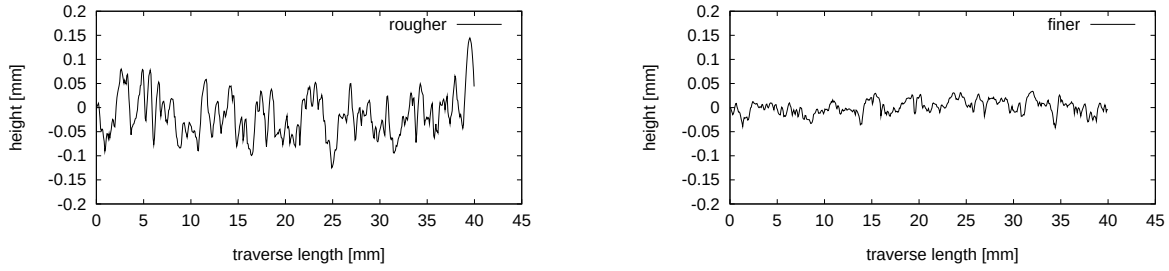

(a) Experimental Part Using Rough Particles (top surface).

(b) Test Part Using Finer Particles (top surface).

Figure 5: Surfaces Profiles: Rough vs. Finer Particle Material.

Changing the powder particle results in an improved surface quality, as shown in Figure 5. For example, the average RMS roughness with the finer powder material is $10\mu m$, instead of around $30\mu m$ with the rougher powder material. In addition to improving the average surface precision, analysis of the surface structure following the design change reveals two additional fault patterns that were initially masked, as shown in Figure 4(b). Spectral analysis is performed on profile measurements designed to isolate the two separate fault patterns. The first pattern shows most visibly in the transverse direction, whereas the second pattern is most visible in the longitudinal direction. As a result, two directions are measured. The corresponding power spectra in the longitudinal and transverse directions are shown in Figure 6.

The spectrum for the longitudinal measurement reveals three frequency components. The dominant frequency component at 0.403 $cycles/mm$ (period of 2.48 mm) corresponds to the frequency of the fault pattern left on the powder surface due to the roller vibration as a new layer is deposited

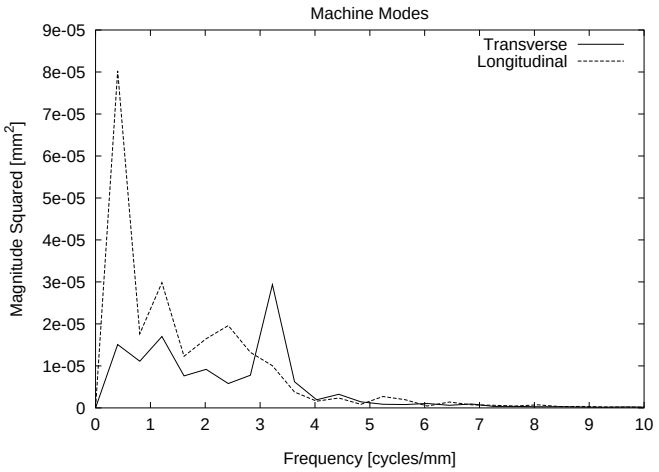

Figure 6: Faults Revealed on Parts Built Using Finer Powder.

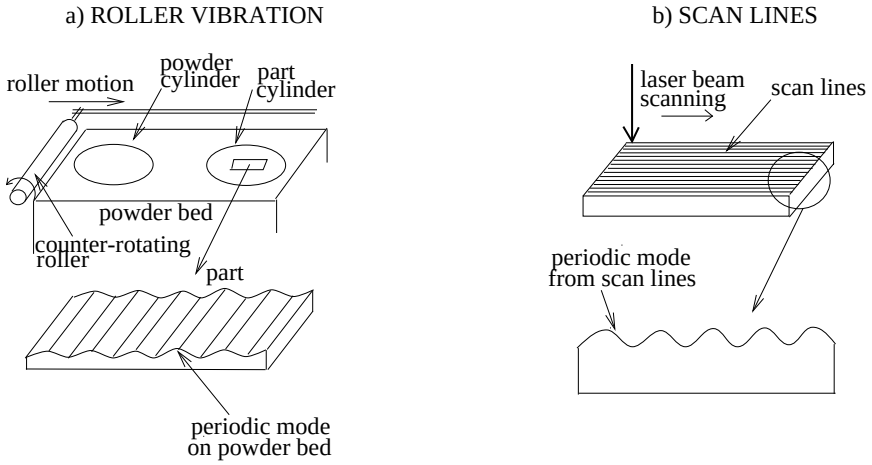

Figure 7: Fault Patterns due to the Roller and the Scanning Mechanisms.

(Figure 7a). Measurement of the period of this fault pattern with a caliper and a stereomicroscope gives a period of approximately equivalent to that detected by the spectrum. Furthermore, the analysis reveals two additional frequency components at frequencies of 1.209 $cycles/mm$ and 2.419 $cycles/mm$. These frequency components should be verified by measuring the vibrations of the roller motion, and studying the relation to the frequency components that we computed from the surface profile measurement. Correlation techniques can be used to accomplish this task. Specific bandwidths can be established to recognize these faults patterns in the future. Controlled experiments studying the roller vibrations and the surface profiles will be conducted later using this new powder material.

The spectrum of the transverse measurement also shows three frequency components. The dominant frequency component at 3.22 $cycles/mm$ (period of 0.31 mm) corresponds to the periodic pattern left on the part surface due to the scan lines of the laser beam (Figure 7b). Again, the measurement of the period of this fault component on the surface agrees with these numbers. The

predicted value of the period of this fault pattern can be derived from the knowledge of the beam width and overlap between scans used when the part was built.

The quantification of these fault patterns provides a means to monitor their occurrence and severity. The frequency is used to monitor when the fault occurs and to determine its origin, whereas the amplitude is used to assess the fault's severity. For example, based on the magnitudes in Figure 6, the fault pattern due to the roller chatter marks is more severe than the pattern due to the beam scan lines. A threshold for fault magnitudes can be set to decide when these fault patterns become important. On the other hand, the frequency of the fault patterns can be used to decide when these faults occur, pointing to a fault in the roller mechanism, for example.

Fault Patterns on Top Surfaces of Angled Parts

In addition to the 0° parts, we also examine the fault patterns introduced on the top surfaces of parts built at different angles (see Figure 2(b)). Recall that the previous analysis of surface precision indicates that part orientation is a significant factor in generating poor quality parts. Surfaces of more complex SLS parts are often built at an angle from the horizontal and vertical axes. The accuracy and surface finish resulting from such surfaces are typically less acceptable than that of the vertically or horizontally oriented surfaces. Therefore, it becomes important to determine the effect of build angle on the surface characteristics of SLS parts. In this portion of the work, we examine the periodic fault pattern introduced by the successive stacking of layers on parts built at an angle from the powder bed; the purpose is to determine the nature of this pattern and assess its severity in order to establish remedial measures. Profiles of the 30°, 45°, and 60° parts from the experiments described earlier are compared to surfaces predicted from a model.

Because SLS is a layered manufacturing process, faces at an angle to the build direction other than 0° or 90° are approximated by a series of "stair-steps," as shown in cross-section in Figure 8(a) and Figure 8(b). Using a coordinate system with one axis placed on the plane being approximated, an error function can be constructed as the distance between the original plane and the discretized facsimile. This function is depicted in Figure 8(c). Clearly, the period and magnitude of the function depend on the layer thickness and the angle of the plane to the build direction. To generate a one-dimensional profile, the following equation is used to model the stair-step effect, also called the aliasing effect:

$$f(x,\theta,t) = \begin{cases} (-\frac{T}{2} - x)\tan(\frac{\pi}{2} - \theta) & x \in [-\frac{T}{2}, -x_c] \\ x\tan(\theta) & x \in [-x_c, x_c] \\ (\frac{T}{2} - x)\tan(\frac{\pi}{2} - \theta) & x \in [x_c, \frac{T}{2}] \end{cases} \quad (5)$$

where x is the distance along the surface, θ is the angle of the surface to the build direction, t is the layer thickness, $x_c = \frac{t\cos(\theta)}{2}$, and, $T = \frac{t}{\cos(\theta)}$ is the period.

The power spectra of parts at three different angles are shown in Figure 9(a). Two dominant frequency components are observed from these plots. The high frequency component observed on these surfaces corresponds to the aliasing effect caused by the layer-by-layer forming of the parts. To assure that this phenomenon is not masked by other errors, the power spectra from the experiments are compared to the power spectrum of an expected profile from the model (Equation 5), as shown in Figure 9(b). The machine used to build these parts repeats each slice; this doubles the effective layer thickness used in the expected profile. Note that the frequency component shifts to a higher frequency with smaller magnitude as the build angle increases, as predicted by the model. In

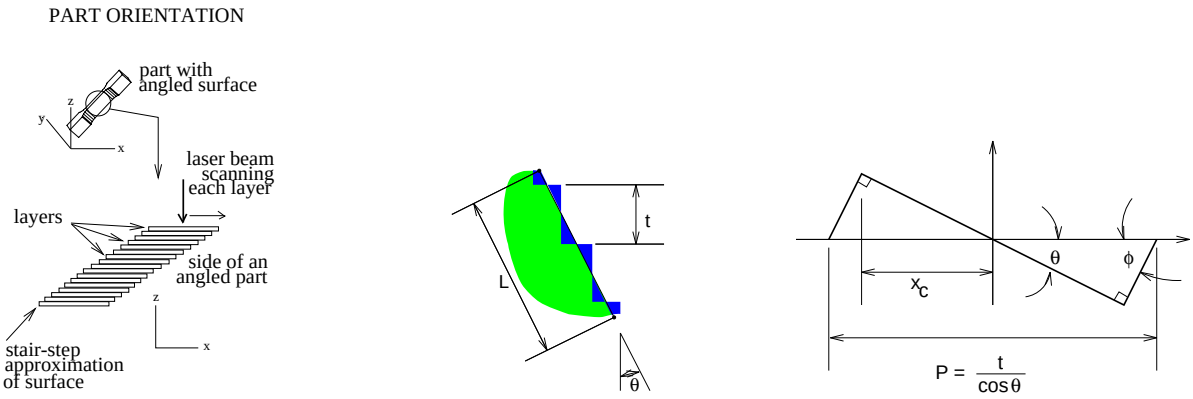

(a) Fault Mechanism on Surfaces of Angled Parts.

(b) Approximation of planar surface (edge on view)

(c) Error function for the surface

Figure 8: Faults on Layered Parts.

addition to verifying that aliasing occurs as predicted, the transformed data make it clear that the magnitude of this effect can dominate other surface errors at build angles near horizontal. This suggests that the angle of large facets to the build direction can significantly affect the surface quality of a part. The aliasing model can be used to minimize surface error by varying part build angle [26].

The spectral analysis also reveals an unpredicted pattern, most visible on the top surfaces of angled parts. The low frequency component, shown in Figure 9(a), is mainly due to the observed shifting of the layers from the motion of the roller, as well as linear trends caused by curl. When the roller shifts the part, the next layer will be offset slightly from the rest of the part, as shown in Figure 10. This appears as a low frequency term in the power spectrum of a segment containing a shift. This effect is shown in the actual profile measurement as a shift at the two end points of the parts built at an angle; it is best observed on 30° parts, as shown in Figure 11(b). In Figure 11(a), the layer-shifting effect shows as a bump on the surface. This picture also shows the stair-step effect discussed earlier.

Identification and Monitoring of Fault Patterns

In the second portion of our approach, we examined surfaces from SLS parts to study the characteristics of individual fault patterns using standard random process analysis methods. As we have shown, the spectral analysis provides sufficient information on the characteristics of the dominant fault patterns on part surfaces, provided that the deterministic patterns on the surfaces are not masked by other fault patterns. Once the nature of the fault patterns are identified by means of formal methods, remedial action can be recommended or automatically implemented based on the insight gained from the spectral analysis of the surfaces of manufactured parts.

We have detected several important fault patterns from this analysis. First, the build orientation of a part introduces a periodic fault component that is easily detected on the surfaces of angled parts using the spectral analysis technique. We have shown that the thickness of the layer used to build the part contributes to the amplitude and frequency of this fault pattern. The results show

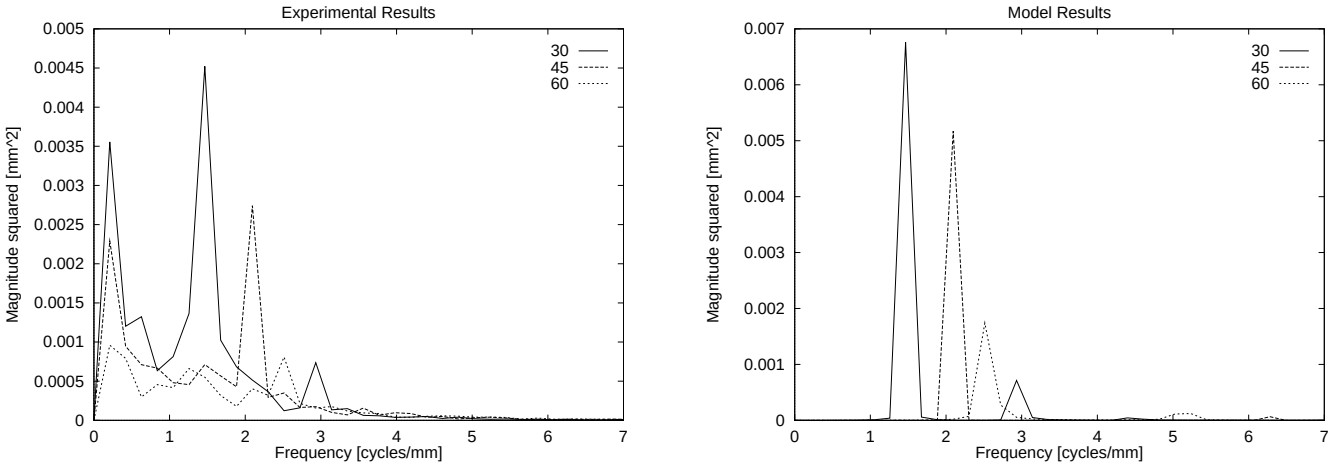

(a) Measured power spectra.

(b) Expected power spectra.

Figure 9: Comparison of Power Spectra for Different Build Angles.

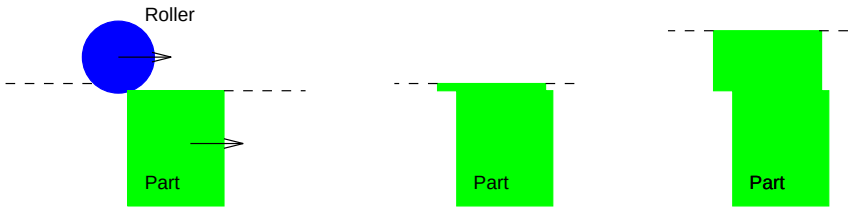

Figure 10: Mechanism for Shifting of Layers.

that increasing the build angle decreases the severity of this fault component. A model of this fault pattern is developed to predict the severity of the fault given the desired orientation and layer thickness. The fault can be minimized using this model. Again using this model, an acceptable threshold for this fault pattern can be preset and then compared to measurements from the surface to monitor the surface quality.

Second, we have shown that patterns due to the rough powder particles dominate the top surfaces of 0° parts. To improve surface precision, parts are formed using a finer powder material. While resulting in improved surface precision, the design change reveals additional surface fault patterns that were initially masked. A sample part using the finer powder material is measured to reveal two periodic fault patterns from roller vibration and from beam scan lines. The marks left from the roller vibrations can be monitored and correlated to the roller vibrations. If an acceptable threshold for the magnitude of these vibrations is established based on the correlation to the magnitude of the fault patterns, the vibrations of the roller can be monitored and remedial action can be recommended if this threshold is exceeded. The marks left on the part due the scan lines can also be monitored to recommend proper beam width and beam overlap parameters based on acceptable fault magnitudes established by the customer. Experiments using this new powder material will be conducted to implement such remedial measures.

In addition to these fault patterns, we also detected an unpredicted spatial fault pattern due

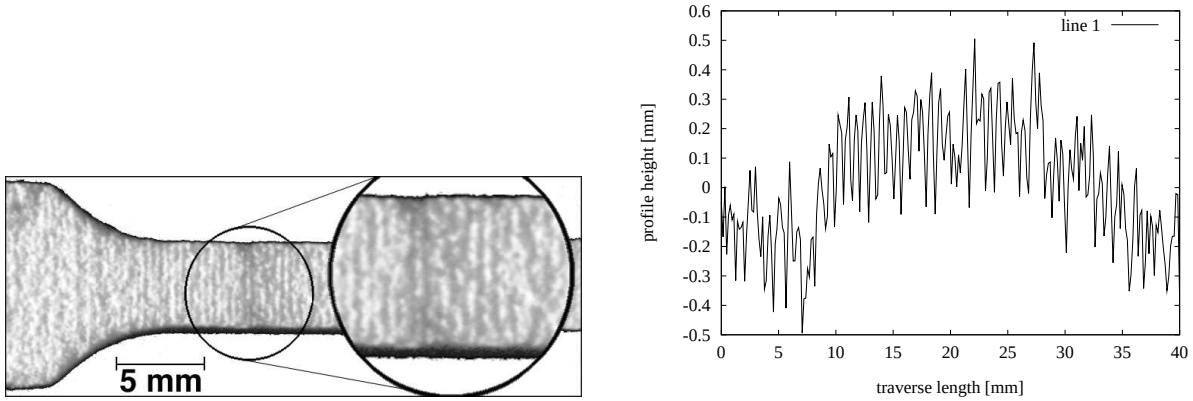

(a) Surface Picture.

(b) Surface Profile Measurement.

Figure 11: Shifting of Layers on a 30-Degree Part.

to layer shifting. A shift in the layers was observed as the roller traveled over each newly-formed layer. The mode was shown to be more severe on the surfaces of parts built at an angle, especially at high power levels. Remedial action needs to be taken to eliminate this mode. Commercial SLS parts are typically built with a number of "tortillas" to remedy this problem. Tortillas are layers with a larger cross-section that prevent the part from being shifted. Shifting is less severe when parts with a larger cross-section are built. The necessity of these layers of larger cross-sectional areas is typically determined by the operator. Using results from analysis methods such as the one presented in this work, the implementation of this remedial action can be automated. For instance, a threshold can be established to indicate acceptable and unacceptable levels of this fault pattern and compared to the actual patterns from the part; remedial action, such as, inclusion of tortillas, or calibration of relevant parameters, can be initiated once the severity of the fault pattern is declared unacceptable.

Conclusions and Future Work

This paper presents experiments designed to characterize the spatial modes that manifest on polycarbonate parts from faults in Selective Laser Sintering (SLS). Experiments are run by varying three parameters: laser power, layer thickness, and build angle with respect to the horizontal powder bed. The surfaces of parts produced from the SLS process are investigated in order to determine the part quality. Part quality can be affected by fault patterns that are generated on surfaces because of various fault-generating mechanisms. This work aims at identifying these mechanisms by using surface analysis tools, along with factorial experimental design and ANOVA tools.

The systematic approach described in this work can be applied to any newly developed manufacturing process to determine the parameters that affect part quality, so that an optimization scheme can be proposed to improve part quality, and to determine the types of faults and their origin so that remedial action can be taken. Such formal means of detecting, quantifying, and characterizing faults in a manufacturing system are necessary to allow for the monitoring and control

of the system to assure the production of improved quality parts.

The main contribution of this work in the layered manufacturing field is to provide an investigation of the types and origins of fault patterns that result in poor quality SLS products. This work is the first attempt to identify the causes of surface errors on SLS parts. Surfaces from Selective Laser Sintering, as well as other signals such as the laser beam position, and surfaces from other manufacturing processes, will be investigated further to determine the various fault patterns during the manufacture of a part. More suitable methods are also being investigated to provide more accurate decomposition of signals into their individual fault components and to determine the origins of these fault patterns. Specifically, the authors are investigating a potential method called the Karhunen-Loève technique. The method has been applied to surfaces from a surface grinding process [27], and is being developed further using surfaces from Selective Laser Sintering and numerically-generated surfaces [12, 28, 29]. Other methods such as higher-order statistics and wavelet transforms are also possible candidates to analyze complex surfaces [30, 31]. The suitability of these methods is currently being studied.

Acknowledgment

This material is based on work supported, in part, by a grant from the Office of Naval Research, the National Science Foundation, an NSF Young Investigator Award, a grant from TARP, plus research grants from Ford Motor Company, Texas Instruments, and Desktop Manufacturing Inc., and the June and Gene Gillis Endowed Faculty Fellowship in Manufacturing. Any opinions, findings, conclusions or recommendations expressed in this publication are those of the authors and do not necessarily reflect the views of the sponsors.

References

[1] S.D. Eppinger, C.D. Huber, and V.H. Pham. A methodology for manufacturing process signature analysis. *Journal of Manufacturing Systems*, 14(1):20–34, 1995.

[2] J. Sottile and L.E. Holloway. An overview of fault monitoring and diagnosis in mining equipment. *IEEE Transactions on Industry Applications*, 30(5):1326–1332, September/October 1994.

[3] C.M. Ho and K.N. Otto. Modeling manufacturing quality contraints for product development. In *Design Engineering Technical Conferences*, volume DE-Vol.83 / 2, pages 483–494, Boston, Ma, September 1995.

[4] A.H. Slocum. *Precision Machine Design.* Prentice Hall, Englewood Cliffs, NJ, 1992.

[5] J.C. Nelson. *Selective Laser Sintering: A Definition of the Process and an Empirical Sintering Model.* PhD thesis, The University of Texas at Austin, May 1993.

[6] P.F. Jacobs. *Rapid Prototyping and Manufacturing: Fundamentals of StereoLithography.* Society of Manufacturing Engineers, New York, 1992.

[7] D.C. Thompson. The optimization of part orientation for solid freeform manufacture. Master's thesis, The University of Texas at Austin, December 1995.

[8] J.J. Beaman. Machine issues associated with solid freeform fabrication. In *SFF Symposium Proceedings*, pages 309–330. The University of Texas at Austin, August 1992.

[9] P. Forderhase. Sinterstation 2000 scanner optimization. Internal document on DOE studies on dimensional accuracy, DTM, Austin, Tx, October 1994.

[10] J.C. Nelson. Scanning method comparison. Internal Document, DTM, Austin, Tx, September 1993.

[11] X. Deng and J.J. Beaman. Application of factorial design in Selective Laser Sintering. In *Solid Freeform Fabrication Symposium*, volume 3, pages 154–160, Austin, TX, August 1992. The University of Texas at Austin.

[12] I.Y. Tumer, D.C. Thompson, R.H. Crawford, and K.L. Wood. Surface characterization of polycarbonate parts from selective laser sintering. In *SFF Symposium Proceedings*, pages 181–188. The University of Texas at Austin, August 1995.

[13] D.J. Whitehouse. *Handbook of Surface Metrology*. Institute of Physics Publishing, Bristol, UK, 1994.

[14] N.K. Vail and J.W. Barlow. Modeling of polymer degradation in SLS. In *SFF Symposium Proceedings*, pages 387–395. The University of Texas at Austin, 1994.

[15] G.E.P. Box and N.R. Draper. *Empirical Model-Building and Response Surfaces*. John Wiley and Sons, New York, 1987.

[16] D.C. Montgomery. *Design and Analysis of Experiments*. John Wiley and Sons, New York, 1991.

[17] S. Wolf and R.N. Tauber. *Process Technology*, volume 1 of *Silicon Processing for the VLSI Era*. Lattice Press, Sunset Beach, California, 1986.

[18] Esterline Federal Products. Surfanalyzer 5000. User's Manual, 1993.

[19] D.J. Whitehouse and K.G. Zheng. The use of dual space-frequency functions in machine tool monitoring. *Measurement Science and Technology*, 3:796–808, 1992.

[20] R.E. DeVor, T.H. Chang, and J.W. Sutherland. *Statistical Quality Design and Control*. Macmillan Co., New York, 1992.

[21] I.Y. Tumer, I.J. Busch-Vishniac, and K.L. Wood. Modeling of dynamic errors caused by the beam delivery system in selective laser sintering. In *SFF Symposium Proceedings*, pages 353–361, Austin, Tx, 1995. The University of Texas at Austin.

[22] J. Peters, P. Vanherck, and M. Sastrodino. Assessment of surface typology analysis techniques. *Annals of the CIRP*, 28(2):539–554, 1979.

[23] H.T. Hingle. A practical method of machine tool condition monitoring by analysis of component surface finish data. In *SPIE Proceedings on Micromachining of Elements with Optical and Other Submicrometer Dimensional and Surface Specifications*, volume 803, pages 108–115, Netherlands, April 1987.

[24] J.S. Bendat and A.G. Piersol. *Random Data: Analysis and Measurement Procedures*. John Wiley & Sons, New York, NY, 1986.

[25] S. Braun. *Mechanical Signature Analysis: Theory and Applications*. Academic Press, London, 1986.

[26] D.C. Thompson and R.H. Crawford. Optimizing part quality with orientation. In *SFF Symposium Proceedings*, pages 362–368, Austin, Tx, August 1995. The University of Texas at Austin.

[27] I.Y. Tumer, R.S. Srinivasan, and K.L. Wood. Investigation of characteristic measures for the analysis and synthesis of precision-machined surfaces. *Journal of Manufacturing Systems*, 14(5):378–392, September/October 1995.

[28] I.Y. Tumer, K.L. Wood, and I.J. Busch-Vishniac. Monitoring fault condition during manufacturing using the Karhunen-Loève transform. In *1997 ASME Mechanical Vibration and Noise Conference, System Health Condition Monitoring Symposium*, Sacramento, California, September 1997.

[29] I.Y. Tumer, K.L. Wood, and I.J. Busch-Vishniac. Improving manufacturing precision using the Karhunen-Loève transform. In *1997 ASME Design for Manufacturing Conference, Integrated Design Symposium*, Sacramento, California, September 1997.

[30] R.W. Barker. *Incipient Fault Detection Using Higher-Order Statistics.* PhD thesis, The University of Texas, Austin, Tx, 1991.

[31] M.D. Ladd. *Detection of Machinery Faults in Noise Using Wavelet Transform Techniques.* PhD thesis, The University of Texas, Austin, Tx, 1995.